

***Ab initio* calculations of structural and magnetic properties of Ni-Co-Mn-Cr-Sn alloys**

Mikhail Zagrebin^{1,2,a}, Vladimir Sokolovskiy^{1,3}, Elizaveta Smolyakova¹ and Vasiliy Buchelnikov¹

¹*Chelyabinsk State University, Condensed Matter Physics Department, 454001 Chelyabinsk, Russia*

²*National Research South Ural State University, Mathematical Physics Equations Department, 454080 Chelyabinsk, Russia*

³*National University of Science and Technology "MIS&S", Moscow, 119049, Russia*

Abstract. The composition dependences of crystal lattice parameters, bulk modulus, magnetic moments, magnetic exchange parameters in $\text{Ni}_{2-y}\text{Co}_y\text{Mn}_{1.5-x}\text{Cr}_x\text{Sn}_{0.5}$ ($y = 0.2, 0.4$; $0.0 \leq x \leq 0.4$) Heusler alloys are investigated with the help of ab initio calculations. Our simulations have shown that crystal lattice parameter firstly increased and then decreased with Cr content (x) increasing. The strongest ferromagnetic interaction for $\text{Ni}_{1.6}\text{Co}_{0.4}\text{Mn}_{1.4}\text{Cr}_{0.1}\text{Sn}_{0.5}$ is nearest-neighbor interaction between Co and Mn₁ (on own sites). The strongest antiferromagnetic interaction is observed between nearest-neighbor Mn₁-Cr atoms in the first coordination sphere and it is equal to -15meV. Total magnetic moment of $\text{Ni}_{2-y}\text{Co}_y\text{Mn}_{1.5-x}\text{Cr}_x\text{Sn}_{0.5}$ ($y = 0.2, 0.4$; $0.0 \leq x \leq 0.4$) takes value in region from $6.1 \mu_B$ to $6.6 \mu_B$.

1 Introduction

Heusler alloys have attracted a great interest because of number of effects (such as shape memory, magnetocaloric effects (MCE), exchange bias and superelasticity) and their potential applications as intelligent functional materials [1, 2]. Recently experimentalists started to study Cr-doped Ni-Co-Mn-Z (Z = In, Sn, Sb) Heusler alloys. The idea of these investigations is that the addition of Cr lead to decreasing of magnetic moment at martensitic state. In this case the large difference between magnetization in austenite and martensite is observed, which lead to the large value of magnetocaloric effect [3, 4]. In [5-7] structural and magnetic properties of Ni-Co-Mn-Cr-In alloys with the help of first principles and Monte-Carlo simulations were investigated. Sokolovskiy et al. show that the substitution of 5% Co for Ni and 5% Cr for Mn results in a first-order magnetostructural transition from ferromagnetic (FM) austenite to antiferromagnetic (AFM) martensite, which is accompanied by a spin-flip transition upon cooling. As a result, a large magnetization drop and giant inverse MCE can be achieved of $\Delta T_{ad} \approx 10$ K in the 2 T field across the magnetostructural phase transition [7].

In this work we present the results of *ab initio* investigations of structural and magnetic properties of austenite of $\text{Ni}_{2-y}\text{Co}_y\text{Mn}_{1.5-x}\text{Cr}_x\text{Sn}_{0.5}$ ($y = 0.2, 0.4$; $0.0 \leq x \leq 0.4$) Heusler alloys.

2 Calculation details

All the calculations were performed using the density functional theory as part of the spin-polarized relativistic

Korringa-Kohn-Rostoker (SPR-KKR) package [8, 9]. This code is based on the KKR-Green's function formalism that makes use of the multiple-scattering theory, and the electronic structure is expressed in terms of the corresponding Green's function as opposed to Bloch wave functions and eigenvalues. In this code, chemical disorder is treated through the coherent potential approximation [9]. The SPR-KKR was used to determine the optimized lattice parameters with L2₁ unit cell which consist of the 4-atoms. In [5-8] has been shown that austenitic phase in Cr-doped alloys has FM ground state. So, we considered FM phase also. In this state all magnetic moments of Ni, Co, Mn and Cr atoms are parallel (Sn atom has small magnetic moment and it has not been taken into account). For the optimized lattice parameter the Heisenberg's magnetic exchange coupling parameters J_{ij} were calculated. The exchange coupling parameters J_{ij} within a real-space approach were calculated using an expression proposed by Liechtenstein et al. [10]. In our calculations we used the generalized gradient approximation for the exchange correlation functional in the formulation of Perdew, Burke and Ernzerhof [11]. We used L2₁ structural phase with space group of Fm3m (225), which consists of four interpenetrating face-centered cubic sublattices. In this structure the Sn atoms occupy the sites (0; 0; 0); Mn occupy (1/2; 1/2; 1/2) ones; Ni and Co atoms are randomly located at the sites (1/4; 1/4; 1/4) and (3/4; 3/4; 3/4). The location of addition of Mn and Cr atoms was assumed to be at Sn-site [12].

^a Corresponding author: miczag@mail.ru

3 Results of the first principles calculations

3.1. Equilibrium lattice parameter

On the Table 1 we can see equilibrium lattice parameter of $\text{Ni}_{2-y}\text{Co}_y\text{Mn}_{1.5-x}\text{Cr}_x\text{Sn}_{0.5}$ alloys in austenite phase for different value of Co excess (y) and of Cr excess (x).

Equilibrium lattice constants firstly increases with Cr excess jumping from 0 to 0.1 and then decreases with increasing of Cr excess. Obtained values of lattice constant were used for further calculations of magnetic properties of $\text{Ni}_{2-y}\text{Co}_y\text{Mn}_{1.5-x}\text{Cr}_x\text{Sn}_{0.5}$ alloys.

Table 1. Calculated equilibrium lattice constants of $\text{Ni}_{2-y}\text{Co}_y\text{Mn}_{1.5-x}\text{Cr}_x\text{Sn}_{0.5}$ alloys in austenite state, Å

	$y=0.2$	$y=0.4$
$x=0.0$	6.030	6.023
$x=0.1$	6.032	6.024
$x=0.2$	6.030	6.022
$x=0.3$	6.028	6.0235
$x=0.4$	6.027	6.016

3.2. Bulk modulus

We also calculated bulk modulus for $\text{Ni}_{2-y}\text{Co}_y\text{Mn}_{1.5-x}\text{Cr}_x\text{Sn}_{0.5}$ ($0 \leq x \leq 0.4$; $y = 0.2, 0.4$) alloys. In Table 2 we present the bulk modulus for different Cr excess (x) and Co excess (y). As we can see, for $\text{Co}=0.2$ bulk modulus has a minimum at $\text{Cr}=0.3$ and this minimum is equal to 140.7 GPa; for $\text{Co}=0.4$ bulk modulus has a minimum at $\text{Cr}=0.2$ and this minimum is equal to 143.5GPa.

Table 2. Calculated bulk modulus of $\text{Ni}_{2-y}\text{Co}_y\text{Mn}_{1.5-x}\text{Cr}_x\text{Sn}_{0.5}$ in austenite state, GPa

	$y=0.2$	$y=0.4$
$x=0.0$	141.8	143.9
$x=0.1$	141.6	143.7
$x=0.2$	141.5	143.5
$x=0.3$	140.7	215.2
$x=0.4$	141.7	243.4

3.3. Magnetic moment

The calculations of partial and total magnetic moments of $\text{Ni}_{2-y}\text{Co}_y\text{Mn}_{1.5-x}\text{Cr}_x\text{Sn}_{0.5}$ alloys have been done by means of the SPR-KKR package. Here and further we will use follow designations such as Mn_1 and Mn_2 . Here, Mn atoms, which are located at regular Mn sublattice, are denoted as Mn_1 , whereas Mn_2 designation corresponds to Mn atoms which occupied the Sn sublattice.

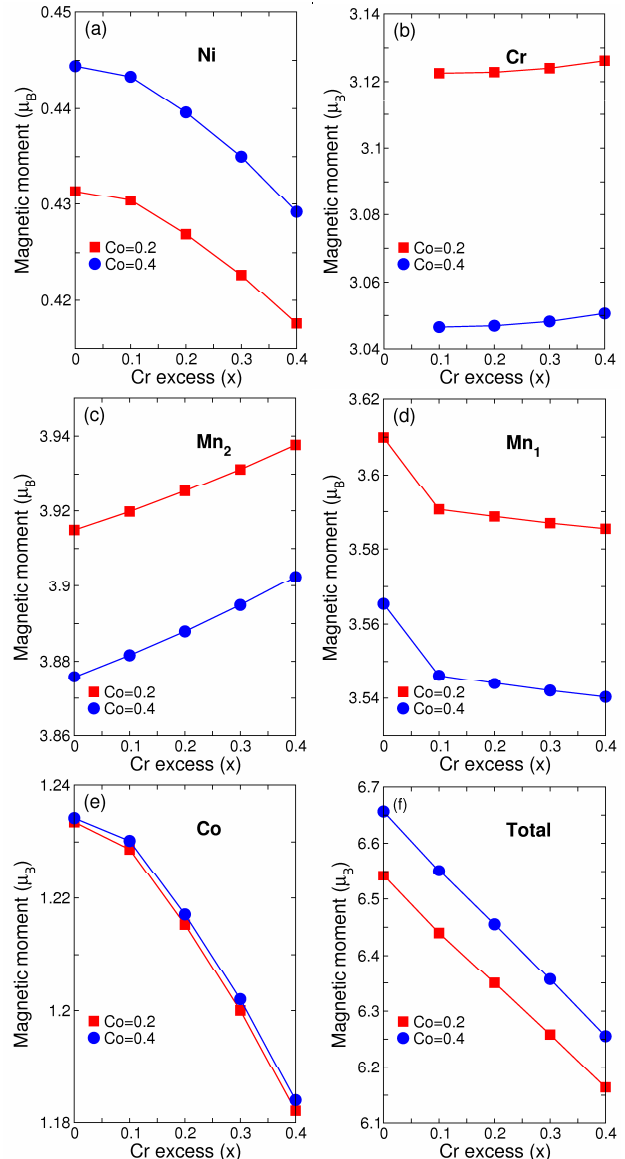


Figure 1: Calculated spin magnetic moment of $\text{Ni}_{2-y}\text{Co}_y\text{Mn}_{1.5-x}\text{Cr}_x\text{Sn}_{0.5}$ alloys in austenite phase for different value of Co excess (y) as a function of Cr excess (x). a) partial magnetic moment of Ni atoms; b) partial magnetic moment of Cr atoms; c) partial magnetic moment of Mn_2 atoms; d) partial magnetic moment of Mn_1 atoms; e.) partial magnetic moment of Co atoms; f) total magnetic moment.

In Fig. 1f we present the composition dependences of the total magnetic moment, whereas partial moments for each sort of atoms as function of Cr excess x is depicted in Fig. 1a – 1e. As we can see from Fig. 1f for zero Cr excess total magnetic moment is $6.55 \mu_B$ and $6.65 \mu_B$ for alloy containing 0.2 and 0.4 of Co respectively. It particularly linearly decreases on $0.4 \mu_B$ with increasing

Cr excess up to 0.4. Concentration dependence of partial magnetic moment of Cr does not depend on Co excess – the difference of Co magnetic moment for two alloys $\text{Ni}_{1.6}\text{Co}_{0.4}\text{Mn}_{1.5-x}\text{Cr}_x\text{Sn}_{0.5}$ and $\text{Ni}_{1.8}\text{Co}_{0.2}\text{Mn}_{1.5-x}\text{Cr}_x\text{Sn}_{0.5}$ distinguish for 1.5%. Partial magnetic moment of Ni increases with increasing of Co, but decreases with increasing of Cr. It's value approximately equal $0.44 \mu_B$. Partial magnetic moment of Mn_1 linearly decreases with increasing of Cr content from $3.57 \mu_B$ to $3.54 \mu_B$ for Co=0.4. In contrast, partial magnetic moment of Mn_2 linearly increases with increasing of Cr.

3.4. Magnetic exchange parameters

Fig. 2 displays the magnetic exchange parameters for $\text{Ni}_{2-y}\text{Co}_y\text{Mn}_{1.5-x}\text{Cr}_x\text{Sn}_{0.5}$ alloys in austenite phase as a function of a distance between pairs of atoms. Here and further, the positive exchange constants ($J_{ij} > 0$) are presented a FM coupling, whereas the negative ones ($J_{ij} < 0$) indicate an AFM coupling. The oscillating damped behavior of J_{ij} can be observed.

The strongest FM interaction for $\text{Ni}_{1.6}\text{Co}_{0.4}\text{Mn}_{1.4}\text{Cr}_{0.1}\text{Sn}_{0.5}$ alloy is nearest-neighbor (NN) interaction between Co and Mn_1 and Co and Mn_2 (Fig. 2a). Note, that value of these interactions are approximately equal to 20 meV and 15 meV respectively. The strongest AFM interaction is observed between NN $\text{Mn}_1\text{-Cr}$ atoms in the first coordination sphere and it is equal to -15meV. This interaction becomes FM at second coordination sphere and then again turns to AFM at third. All other alloys show the same behavior (Fig. 2b, 2c, 2d). It worth mentioning that distance between values of Co-Mn_1 and Co-Mn_2 interactions decreases with increasing Cr excess.

Exchange parameters at the first coordination sphere in austenite state of $\text{Ni}_{2-y}\text{Co}_y\text{Mn}_{1.5-x}\text{Cr}_x\text{Sn}_{0.5}$ alloys as a function Cr excess (x) are depicted in Fig. 3. Most weak interactions from Fig. 2 are not shown. Substitution of Ni instead of Mn_1 or Mn_2 into $\text{Mn}_1\text{-Mn}_2$ turns J_{ij} from AFM state to FM. According to Fig. 3c, 3d, 3f magnetic exchange parameters at the first coordination sphere increases with increasing Co excess and decreases with Cr excess. Whereas, replacing by Co one of atoms from $\text{Mn}_1\text{-Mn}_2$ changes behavioral pattern of J_{ij} – it has bend. $\text{Mn}_1\text{-Co}$ has pronounced maximum 18.9 meV for Co=0.2 and 18.5 for Co=0.4 at Cr=0.1.

4 Summary

The composition dependence of crystal lattice parameters, bulk modulus, magnetic moments and magnetic exchange parameters in $\text{Ni}_{2-y}\text{Co}_y\text{Mn}_{1.5-x}\text{Cr}_x\text{Sn}_{0.5}$ ($0 \leq x \leq 0.4$; $y = 0.2, 0.4$) Heusler alloys are investigated with the help of first principles using the SPR-KKR method. Crystal lattice parameter firstly increased and then decreased with Cr content (x) increasing. The strongest FM interaction for $\text{Ni}_{1.6}\text{Co}_{0.4}\text{Mn}_{1.4}\text{Cr}_{0.1}\text{Sn}_{0.5}$ alloy is nearest-neighbor interaction between Co and Mn_1 . The strongest AFM interaction is observed between NN $\text{Mn}_1\text{-Cr}$ atoms in the first coordination sphere and it is equal to -15meV. Total magnetic moment takes value

in region from $6.1 \mu_B$ to $6.6 \mu_B$. It should be noted that for more complete understanding of crystal and magnetic structure it is necessary to investigate different magnetic structures.

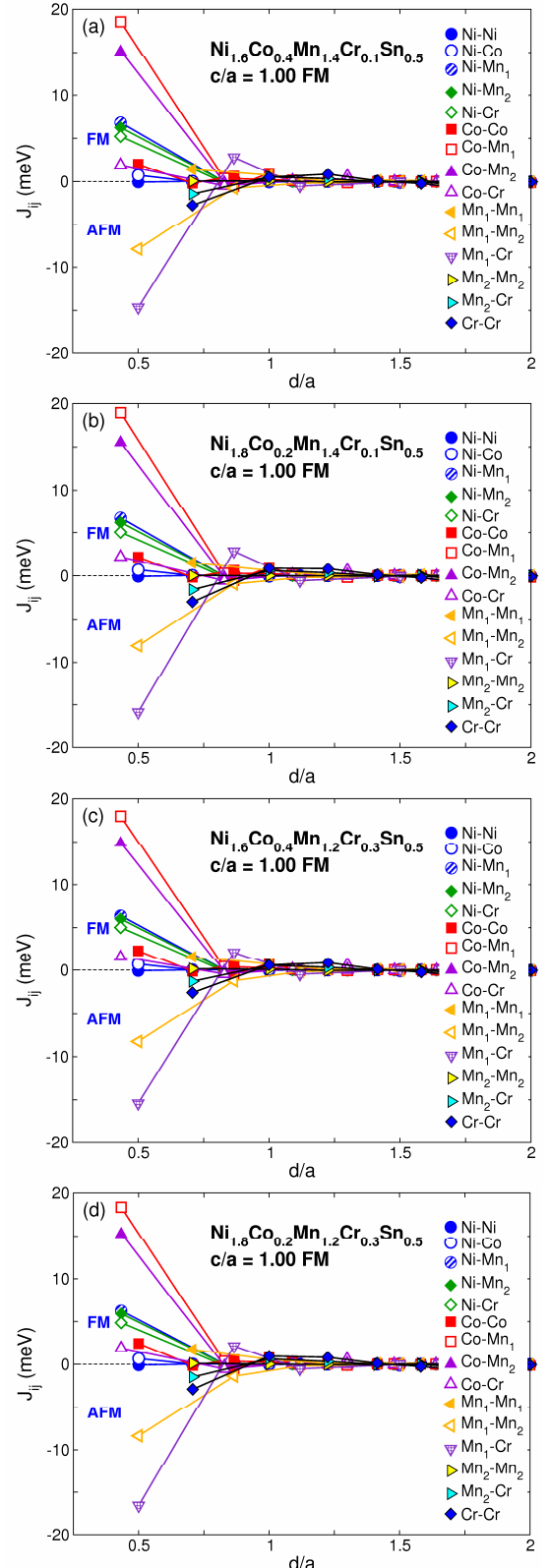


Figure 2: Exchange couplings parameters in austenitic phase for $\text{Ni}_{2-y}\text{Co}_y\text{Mn}_{1.5-x}\text{Cr}_x\text{Sn}_{0.5}$ alloys as a function of a distance between pairs of atoms i and j (in units of the lattice constant a).
 a) $\text{Ni}_{1.6}\text{Co}_{0.4}\text{Mn}_{1.4}\text{Cr}_{0.1}\text{Sn}_{0.5}$; b) $\text{Ni}_{1.8}\text{Co}_{0.2}\text{Mn}_{1.4}\text{Cr}_{0.1}\text{Sn}_{0.5}$; c) $\text{Ni}_{1.6}\text{Co}_{0.4}\text{Mn}_{1.2}\text{Cr}_{0.3}\text{Sn}_{0.5}$; d) $\text{Ni}_{1.8}\text{Co}_{0.2}\text{Mn}_{1.2}\text{Cr}_{0.3}\text{Sn}_{0.5}$.

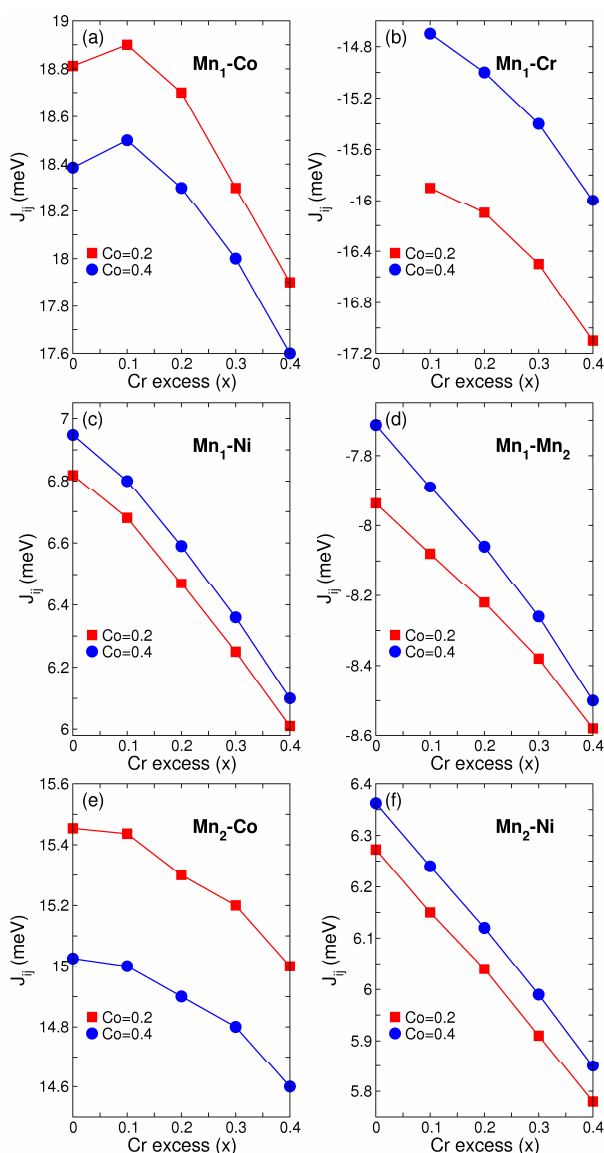


Figure 3: The magnetic exchange parameters J_{ij} in the first coordination sphere for $\text{Ni}_{2-y}\text{Co}_y\text{Mn}_{1.5-x}\text{Cr}_x\text{Sn}_{0.5}$ alloys in austenite phase as a function of Cr excess (x). a) Mn₁-Co coupling; b) Mn₁-Cr coupling; c) Mn₁-Ni coupling; d) Mn₂-Mn₂ coupling; e) Mn₂-Co coupling; f) Mn₂-Ni coupling.

Acknowledgments

This work was supported by Russian Science Fund No. 14-12-00570 (Section 1), Ministry of Education and Science RF No. 3.2021.2014/K (Section 4), RFBR (grants 14-02-01085).

References

- V.D. Buchel'nikov, A.N. Vasiliev, V.V. Koledov, S.V. Taskaev, V.V. Khovailo, and V.G. Shavrov. Phys. Usp. **49**, 871 (2006).
- P. Entel, M.E. Gruner, A. Dannenberg, M. Siewert, S.K. Nayak, H.C. Herper, and V. Buchel'nikov. Mater. Sci. Forum **635**, 3 (2010).
- M.Khan, J. Jung, S.S. Stoyko, A. Mar, A. Quetz, T. Samanta, I. Dubenko, N. Ali, S. Stadler, and K.H. Chow. Appl. Phys. Lett., **102**, 112402 (2013).
- M. Khan, J. Jung, S.S. Stoyko, A. Mar, A. Quetz, T. Samanta, I. Dubenko, N. Ali, S. Stadler, and K.H. Chow Appl. Phys. Lett., **100**, 172403 (2012).
- V. Sokolovskiy, V. Buchel'nikov, P. Entel, M. Gruner IEEE Transactions on Magnetics, doi: 10.1109/TMAG.2015.2439391
- V.D. Buchel'nikov, V.V. Sokolovskiy, M.E. Gruner, P. Entel. IEEE Transactions on Magnetics. doi: 10.1109/TMAG.2015.2438953
- V.V. Sokolovskiy, P. Entel, V.D. Buchel'nikov, and M. E. Gruner. Phys. Rev. B. **91**, 220409(R) (2015).
- H. Ebert. SPRKKR package (version 6.3). <http://ebert.cup.uni-muenchen.de/>.
- H. Ebert, D. Koderitzsch, and J. Minar. Rep. Prog. Phys., **74**, 096501 (2011).
- A.I. Liechtenstein, M.I. Katsnelson, V.P. Antropov, and V.A. Gubanov. J. Magn. Magn. Mater. **67**, 65 (1987).
- J.P. Perdew, K. Burke, and M. Ernzerhof. Phys. Rev. B. **77**, 3865 (1997).
- V.D. Buchel'nikov, V.V. Sokolovskiy, M.A. Zagrebin, M.A. Klyuchnikova, P. Entel. J. Magn. Magn. Mater. **383**, 180 (2015).